Stochastic Optimization of a Multi-Carrier Energy System with the Participation of Renewable Energy Sources and Integrated Demand Response Programs

Mohammad amin Babajani-Chari, Ali Ghasemi-Marzbali*

Department of Electrical and Biomedical Engineering, Mazandaran University of Science and Technology, Babol, Iran

*Corresponding author: ali.ghasemi@ustmb.ac.ir

Abstract: In modern engineering, optimizing energy hub-based microgrids that incorporate renewable energy resources to meet both electrical and thermal demands presents a significant challenge. This study focuses on the stochastic optimization of a multi-carrier energy microgrid, integrating renewable energy sources to enhance efficiency and reduce operational costs. A demand response program is employed to optimize the allocation of costs and improve the load profiles for both electricity and thermal energy. To address the uncertainty of renewable resources, a scenario-based planning approach is implemented to reduce the impact of variability. The model schedules energy production and consumption for a 24-hour period, with objective functions targeting energy purchase costs, fuel costs, profits from energy sales, and greenhouse gas emission reduction. The proposed methodology is tested on a sample microgrid system using Python solvers for optimization. Results, analyzed under various scenarios, show a significant reduction in costs when compared to conventional systems. Specifically, the total cost for meeting electrical and thermal demands through the traditional electricity and gas network is 279,910 cents, while the optimized system reduces the cost to 164,682 cents, yielding a savings of approximately 41%. These findings highlight the effectiveness of the proposed optimization model in reducing both costs and environmental impact.

Keywords: Multi-Carrier Energy – Stochastic Optimization – Demand Response – Microgrid – Renewable Energy Sources.

Nomencalature

CHP	Combined Heat and Power
DER	Distributed Energy Resources
DRP	Demand Response Program
EEG	Electrical Energy Grids
EESS	Electrical Energy Storage System
EV	Electric Vehicle
FGR	Flue Gas Recirculation
IBDR	IncentiveBased Demand Response
MG	Microgrid
MILP	Mixed Integer Linear Programming
MPC	Model Predictive Control
NG	Natural Gas
OPF	Optimal Power Flow
P2P	Peer-to-Peer
PHEV	Plug-in Hybrid Electric Vehicle
PV	Photovoltaic
SOC	State of Charge
TE	Transactive Energy
V2G	VehicletoGrid
WT	Wind Turbine

Variables and parameters

λ_e, λ_g	Electricity, gas and price

λ_g^{ST}	Electrical storages operation cost
λ_{cr}^{DR}	Electrical/Thermal DR operation cost
DR_{cr}	Rate of load reduction in electrical/thermal DRP
$Load$	Load after DRP
L_{inc}	Increased load in DRP
$DR^{\max}$	Maximum rate of load reduction
γ_{CHP}, γ_B	CO_2 emission factor of CHP and boiler
γ_e, γ_g	CO_2 emission factor of electricity and gas network
D_e, D_h	Electrical and heat demand
η	efficiency
$\eta_e^{CHP}, \eta_h^{CHP}$	Gas to electricity and heat efficiency for CHP
η_h^B	Gas to heat efficiency for Boiler
η_e^T, η_h^C	Transformer and converter efficiencies
$SoC_b^{\min}$	Minimum state of charging battery b (KWh)
$SoC_b^{\max}$	Maximum state of charging battery b (KWh)
$P_{ch,b}(t)$	Charging power of battery at time t (KW)
$P_{dich,b}(t)$	Discharging power of battery at time t (KW)
$SoC_b(t)$	State of charge of battery b (KWh)
$X_{ch,b}(t)$	Binary variable for charging of battery b
$X_{dich,b}(t)$	Binary variable for discharging of battery b

$P_{ch,b}^{\max}$	Maximum charging power battery b (KW)
$P_{dich,b}^{\max}$	Maximum discharging power battery b (KW)
E_b	Capacity of battery b (KWh)
η_c	Charging efficiency of battery b (%)
η_d	discharging efficiency of battery b (%)
P_w^{out}	Wind turbine rated power
w	Wind speed
$w_o^{cut}, w_i^{cut}, w_r^w$	Cut out, cut in and rated wind speed
T_{cell}	cell temperature (°C)
T_{amb}	ambient temperature (°C)
k_s	solar clearness (kW/m^2)
k_v, k_1	current-temperature coefficient (mA/°C)
N_{OT}	rated operating temperature of PV cell (°C)
V_{OC}	open-circuit voltage (V) of the PV module
I_{SC}	short-circuit current (A) of the PV module
V_{PV}	output voltage of the PV module (V)
I_{PV}	output current of the PV module (A)
G_t	solar irradiance on a horizontal plane (kW/m^2)
N_{PV}	number of PV modules
α, β	parameters of the beta PDF

$f_b(r)$	Beta PDF for solar irradiance r
$f_w(v)$	Rayleigh PDF for wind speed v
P_e	Amount of purchased electricity from electrical network
P_g	Amount of purchased natural gas from gas network
P_g^{CHP}	Amount of natural gas entering to the CHP
P_g^B	Amount of natural gas entering to the boiler
P_{PV}	Electrical power generated by PV
P_{WT}	Electrical power generated by WT
$Load$	Load after DRP

1- Introduction

The rapid modernization of countries has significantly increased electricity demand, surpassing the capacities of conventional energy sources such as coal and gas, thereby exerting a detrimental impact on the environment [1]. To mitigate this issue, there is a notable shift towards RER to fulfill energy needs. Concurrently, energy hubs have emerged as pivotal infrastructures, integrating diverse energy carriers to meet varying load requirements [2]. These hubs manage inputs such as electricity, natural gas, and water, and produce outputs including electrical, thermal, cooling, and hot water energies. They comprise generation technologies (e.g., wind turbines, solar panels), energy conversion devices (e.g., boilers, CHP units, heat pumps), and energy storage systems (e.g., electrical and thermal storage) [3]. Optimizing the management of an energy hub is challenged by uncertainties at both input and output levels [4]. These uncertainties encompass fluctuating electricity prices, unpredictable natural gas supplies, and the variable output of renewable energy

sources [5]. Furthermore, accurately forecasting demands for electrical, thermal, and cooling loads contributes to the complexity [6]. The interaction between inputs and outputs, such as how energy hub outputs influence energy prices, further complicates the optimal planning of microgrids [7]. Recent years have seen a surge in studies investigating these topics, which are comprehensively reviewed below [8]. In [9], the deregulation of EEGs and the shift to distributed wind generation introduce operational challenges. Integrating DRPs further complicates multi-area EEG management. A method is proposed to enhance grid security by leveraging DRPs and mitigating wind energy fluctuations through coordinated EESSs. In [10], cost-effective scheduling of distributed energy resources using advanced optimization algorithms is a key focus in microgrid energy management. Load-shifting techniques, often combined with constraints like PHEV scheduling and battery life assessment, aim to enhance efficiency, though emission reduction is rarely prioritized. To address this, an IBDR is introduced to encourage load curtailment during peak hours, rewarding participants while reducing emissions and generation costs. In [11], the electrification of transportation in MGs is highlighted as a key solution to global warming, fossil fuel depletion, and the demand for clean energy. V2G technology enables efficient EV integration into power grids. To address uncertainties in EV charging, renewable generation, load demand, and market prices, the unscented transform is applied. The problem is formulated as a constrained single-objective optimization, minimizing MG operational costs while ensuring practical feasibility. In [12], the integration of cogeneration plants and energy conversion facilities introduces both opportunities and challenges in energy system management. Understanding the complex interactions in multi-carrier energy systems requires advanced mathematical models. This study examines a thermal and electrical energy distribution system from a market perspective, incorporating network losses using a nonlinear optimal AC load distribution model.

In [13], a hybrid optimization framework was developed for multi-energy microgrids, integrating renewable sources, storage systems, and flexible loads. The study employed a multi-objective optimization approach to minimize operational costs and maximize renewable utilization. A stochastic modeling technique was used to handle uncertainties in energy generation and demand fluctuations. A game-theoretic approach for P2P energy trading in smart grids was proposed in [14], focusing on decentralized energy transactions. The model considered user preferences, dynamic pricing, and grid constraints to optimize energy exchanges among prosumers. In [15], a demand response-based scheduling strategy was introduced to optimize microgrid operations while maintaining grid stability. The approach integrated real-time pricing mechanisms and load forecasting techniques to shift peak loads efficiently. The study also analyzed the impact of different demand response programs on cost reduction and system reliability. A robust optimization framework for energy storage scheduling in hybrid renewable systems was presented in [16]. The study accounted for uncertainties in wind and solar power generation using a two-stage stochastic programming approach. The optimization model balanced energy supply and demand while minimizing battery degradation costs. The proposed method demonstrated improved energy reliability and cost-effectiveness in microgrid operations.

In [17], a V2G optimization strategy was explored to enhance grid stability and energy efficiency. The study formulated a bi-level optimization model, considering EV owners' charging preferences and grid operator constraints. The method leveraged real-time energy pricing to maximize economic benefits for both EV owners and the grid. A novel approach to hybrid renewable energy system optimization was introduced in [18], incorporating wind, solar, and hydrogen storage. The study applied a metaheuristic optimization algorithm to minimize energy costs while maximizing system reliability. The proposed method also considered hydrogen production as an auxiliary

energy source to enhance system flexibility. Comparative analysis with conventional optimization techniques highlighted superior performance in cost savings and energy efficiency. In [19], a dynamic energy management model for smart grids was proposed, integrating distributed energy resources and demand-side management strategies. The study used a reinforcement learning-based approach to optimize energy distribution and reduce peak loads. The method accounted for uncertainties in load demand and renewable generation, ensuring real-time adaptability. A multi-objective optimization framework for CHP systems was presented in [20], balancing economic and environmental considerations. The study employed a Pareto-based evolutionary algorithm to optimize energy dispatch and emissions reduction. The proposed model was tested on various industrial and residential CHP configurations. In [21], an IBDR model was developed to encourage load curtailment in microgrids. The study introduced a market-driven approach where consumers were rewarded for reducing consumption during peak hours. A pricing mechanism was formulated to balance supply-demand dynamics while ensuring economic feasibility. The proposed IBDR strategy demonstrated significant cost savings and emission reductions in microgrid operations.

A hierarchical control strategy for DERs in microgrids was proposed in [22], addressing operational efficiency and stability. The model included primary, secondary, and tertiary control layers to manage voltage fluctuations and power balance. The study applied a MPC technique to optimize energy dispatch. In [23], a hybrid artificial intelligence-based forecasting model was developed for renewable energy prediction in smart grids. The approach combined deep learning and statistical techniques to enhance forecasting accuracy. The model was tested on real-world wind and solar energy datasets, demonstrating high precision in energy generation predictions. A risk-based optimization framework for energy management in islanded microgrids was introduced in [24]. The study considered uncertainties in renewable generation and load demand, applying a

scenario-based stochastic optimization technique. The proposed method aimed to minimize energy costs while ensuring reliability under uncertain conditions. In [25], a transactive energy management system was developed for smart grids, enabling decentralized energy trading among consumers and prosumers. The study introduced a blockchain-based market mechanism to ensure secure and transparent transactions. The proposed model optimized energy exchanges using a multi-agent reinforcement learning approach.

A novel OPF model incorporating distributed generation and battery storage was presented in [26]. The study formulated a convex optimization problem to minimize total energy costs while maintaining system reliability. The model accounted for grid constraints and dynamic energy pricing. Simulation results demonstrated that integrating storage systems significantly enhanced grid flexibility and cost-effectiveness. In [27], a multi-layer optimization approach for hybrid energy systems was introduced, integrating demand response and distributed storage. The model utilized a combination of heuristic algorithms and MILP to optimize energy dispatch. The study analyzed multiple case studies with varying load profiles and energy sources. A comprehensive study on the impact of electric vehicle charging on grid stability was conducted in [28]. The study employed a probabilistic modeling technique to assess different EV charging scenarios. The proposed strategy incorporated smart charging techniques to reduce grid congestion and peak demand. Findings suggested that managed EV integration could significantly enhance grid stability and efficiency. In [29], an adaptive energy pricing mechanism was introduced for demand-side management in smart grids. The study proposed a real-time pricing model that dynamically adjusted rates based on energy availability and consumer demand. The approach leveraged machine learning techniques to predict demand fluctuations and optimize pricing strategies. A resilience-based optimization framework for microgrids was developed in [30],

focusing on energy security during extreme events. The model incorporated backup generation, battery storage, and demand response to enhance system reliability. A robust optimization technique was applied to handle uncertainty in renewable generation and load demand. In [31], a coordinated control strategy for hybrid AC/DC microgrids was proposed, integrating renewable energy and storage systems. The study introduced a decentralized control architecture to manage energy flows between AC and DC subsystems. The method leveraged adaptive droop control techniques to maintain voltage stability. A market-driven energy management framework for multi-energy systems was presented in [32], considering electricity, heat, and gas networks. The study formulated a mixed-integer programming model to optimize cross-sector energy exchanges. The proposed approach aimed to minimize total operational costs while ensuring system reliability. Findings suggested that coordinated multi-energy management could significantly enhance system efficiency and cost-effectiveness.

Several scientific gaps persist in the optimization and management of multi-carrier energy microgrids, particularly in handling uncertainties associated with renewable energy sources, integrating demand response programs, and ensuring cost-effective operation:

i) Previous studies have explored various aspects of energy hub optimization, yet many challenges remain unresolved. One significant gap lies in the stochastic modeling of multi-carrier energy systems. While past research has incorporated probabilistic techniques to address uncertainties in renewable energy generation, demand fluctuations, and market prices, many studies have relied on simplified models that fail to capture the full complexity of real-world microgrids. This study advances the field by employing a comprehensive scenario-based approach for uncertainty modeling, thereby improving the robustness and accuracy of energy scheduling strategies. Another gap concerns the integration of DRPs in energy hub optimization.

ii) While existing works have investigated the role of demand-side management in reducing peak loads and operational costs, they often neglect the intricate interaction between electrical and thermal loads within an energy hub framework. This paper introduces a coordinated optimization model that effectively incorporates both electrical and thermal demand response programs, thereby enhancing system flexibility and cost efficiency.

iii) Additionally, previous research has largely focused on single-objective optimization approaches, prioritizing either cost minimization or emission reduction. However, such methods often lead to suboptimal trade-offs between economic and environmental objectives. This study addresses this limitation by formulating a multi-objective optimization problem that simultaneously minimizes energy purchase costs, fuel expenses, and greenhouse gas emissions. By doing so, the proposed model ensures a more balanced and sustainable energy management strategy.

iv) Moreover, the majority of existing works rely on deterministic scheduling techniques, which are less effective in handling the dynamic nature of renewable energy systems. This study overcomes this shortcoming by implementing a 24-hour ahead scheduling framework that accounts for various uncertainties, offering a more adaptive and realistic approach to energy management. Lastly, the validation of optimization models is often overlooked in prior studies, with many relying solely on theoretical simulations without real-world applicability. This paper bridges this gap by implementing the proposed model in a Python-based software environment using advanced solvers.

Here's a concise summary of the main contributions and novelties of your paper:

i. Proposes a comprehensive stochastic optimization framework for an energy hub-based microgrid integrating renewable energy sources.

ii. Introduces a scenario-based approach for handling the uncertainty of renewable energy generation, enhancing the robustness of system planning.

iii. Implements a demand response strategy to optimize cost allocation and improve the load profile for both electrical and thermal demands.

iv. Develops a short-term scheduling model with multiple objective functions, including energy purchase costs, fuel costs, revenue from energy sales, and greenhouse gas emission reduction.

v. Utilizes Python solvers for numerical analysis and validation of the proposed model, ensuring practical applicability.

2. Problem Modeling

This section focuses on the mathematical modeling of the problem based on the set objectives.

2.1. Combined Heat and Power

CHP systems, also known as cogeneration, integrate electricity generation with heat production. These systems, which have been available for several decades, typically use a reciprocating engine or a combustion turbine as the main driver, often fueled by natural gas. The primary advantage of CHP is its efficiency. The system produces electricity alongside heat from the main driver, utilizing both outputs effectively. However, any greenhouse gases emitted by the CHP system must be accounted for, and the microgrid must continually balance demand against costs. This involves determining the difference between the cost of grid electricity and natural gas at any given time, a concept also referred to as "spark spread." Similarly, understanding the trade-off between heat output and electricity generation is crucial for deciding when to purchase additional electricity from the utility and when to sell excess power back to the grid [33]:

$$P_e^{\mathrm{CHP}}(t) = \eta_e^{\mathrm{CHP}} \cdot P_g^{\mathrm{CHP}}(t) \quad (1)$$

$$P_h^{\mathrm{CHP}}(t) = \eta_h^{\mathrm{CHP}} \cdot P_g^{\mathrm{CHP}}(t) \quad (2)$$

where, Equation (1) defines the CHP's electrical output power, while Equation (2) defines its thermal output power. As depicted in Figure 1, the CHP's feasible operating region is outlined by a polygon with four key points. Points A and B signify the maximum electrical and thermal outputs, respectively, with their connecting segment showing the maximum fuel consumption. Conversely, points C and D denote the minimum electrical and thermal outputs, with their connecting segment indicating the minimum fuel consumption. The segments connecting points A to D and B to C establish the operating ranges for power production and maximum heat generation, respectively. Equations (3) and (4) always hold for the production of heat and electricity [34]:

$$P_h^{\mathrm{CHP,min}} \le P_h^{\mathrm{CHP}}(t) \le P_h^{\mathrm{CHP,max}} \quad (3)$$

$$P_e^{\mathrm{CHP,min}} \le P_e^{\mathrm{CHP}}(t) \le P_e^{\mathrm{CHP,max}} \quad (4)$$

Place of Figure 1

2.2. Boiler

A boiler, or steam generator, consists of a series of tubes used to transfer heat from the combustion process to a fluid, ultimately producing hot water or steam. The produced steam or hot water is then compressed and used for applications such as heating. Equation (5) calculates the FGR rate [35]:

$$\mathrm{FGR}(\%) = \frac{\text{Recycled flue gas}}{\text{Total flue gas}} \times 100 \quad (5)$$

The "input-output method" formula is used to determine the boiler efficiency. The unit for total flue gas is kg/hr. Boiler efficiency can be calculated using the output energy and the available input heat with Equation (6), and the thermal power output of the boiler is calculated using Equation (7) [33]:

$$\eta_h^{\mathrm{B}} = \frac{E_o}{E_i} \times 100 \tag{6}$$

$$P_h^{\mathrm{B}}(t) = \eta_h^{\mathrm{B}} \cdot P_g^{\mathrm{B}}(t) \tag{7}$$

2.3. Solar Panel

Determining whether renewable energies are feasible for a specific facility depends on factors such as availability, costs, policies, incentives, local market conditions like electricity pricing, and regulations. For microgrids, solar energy can be a good option as it maximizes consumption. However, generating 1 megawatt of solar power requires approximately 4-5 hectares of space. For those with available rooftop or land space, the decreasing cost of solar panels makes them an attractive choice. The power output of PV systems is inherently uncertain, often modeled using the Beta distribution. The mean (μ) and standard deviation (δ) of solar radiation are used in the model [33]:

$$f_b(r) = \begin{cases} \dfrac{\Gamma(\alpha+\beta)}{\Gamma(\alpha)\Gamma(\beta)} \cdot r^{\alpha-1}(1-r)^{\beta-1}, & 0 \le r \le 1, \alpha \ge 0, \beta \ge 0 \\ 0, & \text{otherwise} \end{cases} \tag{8}$$

$$\alpha = \frac{\mu \cdot \beta}{1-\mu} \tag{9}$$

The Beta distribution function is given by:

$$\beta = (1-\mu) \cdot \left(\frac{\mu \cdot (1+\mu)}{\delta^2} - 1 \right) \tag{10}$$

The electrical energy output of a PV system is calculated using equations (11) to (14), which depend on ambient temperature and solar radiation [36]:

$$T_{\text{cell}} = T_{\text{amb}} + \left(G_t \cdot \frac{N_{OT} - 20}{800} \right) \tag{11}$$

$$V_{\text{PV}} = V_{\text{oc}} - K_v \cdot T_{\text{cell}} \tag{12}$$

$$I_{\text{PV}} = k_s \cdot \left(I_{\text{sc}} + (T_{\text{cell}} - T_{\text{amb}}) \cdot K_1 \right) \tag{13}$$

$$P_{\text{PV}} = N_{\text{PV}} \cdot I_{\text{PV}} \cdot V_{\text{PV}} \cdot \eta \tag{14}$$

2.4. Wind Turbine

Wind power can be a promising choice, but large turbines need to be placed sufficiently away from existing structures to avoid noise and safety issues that could make grid integration challenging. Smaller vertical wind turbines can be installed on rooftops. Consistent good wind conditions are crucial. Like solar panels, connecting to the power grid for selling excess energy is an option. Wind power uncertainties are represented through the Rayleigh distribution, which is derived from the Weibull distribution. The function for the Rayleigh distribution is expressed as follows [37]:

$$f_{\omega}(v) = \frac{k}{c} \left(\frac{v}{c} \right)^{k-1} \exp\left[-\left(\frac{v}{c} \right)^{k} \right] \tag{15}$$

where c is the scale parameter equal to $\frac{2}{\sqrt{\pi}} v_{avg}$, and v_{avg} is the average wind speed at a specific location. The electrical power output of a wind turbine is calculated by [33]:

$$P_W(t) = \begin{cases} 0, & \omega(t) \le \omega_i^{\text{cut}} \text{ or } \omega(t) \ge \omega_o^{\text{cut}} \\ P_W^{\text{out}} \cdot \dfrac{\omega(t) - \omega_i^{\text{cut}}}{\omega_r^w - \omega_i^{\text{cut}}}, & \omega_i^{\text{cut}} \le \omega(t) \le \omega_r^w \\ P_W^{\text{out}}, & \omega_r^w < \omega(t) < \omega_o^{\text{cut}} \end{cases} \tag{16}$$

The power generation curve of the wind turbine is illustrated in Figure 2. These regions are as follows:

Area 1: Cut-in Region ($\omega(t) \le \omega_i^{\text{cut}}$):

- In this range, the wind speed is too low to generate sufficient torque to start the turbine. Thus, the power output remains zero.

Area 2: Partial Load Region ($\omega_i^{\text{cut}} \le \omega(t) \le \omega_r^{\text{w}}$):

- In this region, the turbine begins generating power. The output power increases non-linearly with wind speed, typically following a cubic relationship until the rated wind speed is reached.

Area 3: Rated Power Region ($\omega_r^{\text{w}} < \omega(t) < \omega_o^{\text{cut}}$):

- The wind turbine operates at its maximum power output, P_W^{out}, as it reaches its rated wind speed. The power remains constant in this range.

Area 4: Cut-out Region ($\omega(t) \ge \omega_o^{\text{cut}}$):

- If wind speeds exceed the cut-out threshold, the turbine is shut down to prevent mechanical damage, leading to zero power output.

Place of Figure 2.

2.5. Electrical Energy Storage System

Having on-site energy storage offers several benefits for a microgrid. Firstly, it enhances grid reliability by working in tandem with renewable energy sources. Secondly, it maximizes the value of renewable energy by storing excess energy for use when solar or wind resources are unavailable. Finally, stored energy can manage peak demand, reducing the reliance on the grid during expensive

energy periods. Energy storage is particularly effective for handling load peaks. The operation of energy storage is described by the following equations:

$$\mathrm{SoC}_b(t+1) = \mathrm{SoC}_b(t) + \left(\frac{\eta_c P_{\mathrm{ch.b}}(t)}{E_b} - \frac{P_{\mathrm{disch.b}}(t)}{\eta_d E_b} \right) \tag{17}$$

$$0 \le P_{\mathrm{ch.b}}(t) \le X_{\mathrm{ch.b}}(t) \cdot P_{\mathrm{ch.b}}^{\mathrm{Max}} \tag{18}$$

$$0 \le P_{\mathrm{disch.b}}(t) \le X_{\mathrm{disch.b}}(t) \cdot P_{\mathrm{disch.b}}^{\mathrm{Max}} \tag{19}$$

$$\mathrm{SoC}_b^{\mathrm{Min}} \le \mathrm{SoC}_b(t) \le \mathrm{SoC}_b^{\mathrm{Max}} \tag{20}$$

$$X_{\mathrm{ch.b}}(t) + X_{\mathrm{disch.b}}(t) \le 1 \tag{21}$$

Equation (17) shows the battery charge state. Equations (18) and (19) specify the maximum charge and discharge rates. Equation (20) defines the maximum and minimum storage limits. Equation (21) prevents simultaneous charging and discharging of the storage system.

2.6. Objective Function

The proposed system is framed as a bi-objective optimization challenge. The primary goal is to reduce the total operational expenses of the energy system, as detailed in Equation (22). This objective encompasses costs related to electricity, natural gas, the operation of energy storage systems, and demand response programs for both electrical and thermal energy. The secondary goal, outlined in Equation (23), focuses on minimizing greenhouse gas emissions produced by the energy hub and associated networks. This emissions function has two key components: the first component deals with greenhouse gases emitted from the operation of equipment within the energy hub, such as CHP units and boilers. The second component addresses emissions associated with energy production and transmission across the networks that supply the energy hub:

$$Z_1 = \sum_{t=1}^{24} \left[\begin{array}{l} \lambda_e(t)P_e(t) + \lambda_g(t)P_g(t) + \lambda_e^{ST}(t)\left(P_{\text{ch.b}}(t) + P_{\text{disch.b}}(t)\right) + \\ \sum_{cr\in\{e,h\}} \lambda_{cr}^{DR}(t)\left(L_{inc,cr}(t) + R_{cr}(t)\cdot D_{cr}(t)\right) \end{array} \right] \quad (22)$$

$$Z_2 = \sum_{t=1}^{24} \left[\gamma_{\text{CHP}} P_g^{\text{CHP}}(t) + \gamma_B P_g^B(t) + \gamma_g P_g(t) + \gamma_e P_e(t) \right] \quad (23)$$

The objective function is solved using the weighted sum method, where w_1 and w_2 are the coefficients for the objective functions, both assigned a value of 0.5. This implies that both objectives are considered to have equal importance. The relationship between these coefficients is given by the following equation:

$$\text{Min } OF = w_1 Z_1 + w_2 Z_2 \quad (24)$$

$$w_1 + w_2 = 1 \quad (25)$$

2.7. Electrical Power Balance

Maintaining equilibrium in an energy system requires that production and consumption are always matched. The constraints for balancing electricity, gas, and heat are detailed in Equations (26) through (28). In these constraints, incoming power is denoted by a positive sign, while outgoing power is indicated with a negative sign:

$$D_e(t) = \eta^T P_e(t) + \eta^C \left(P_W(t) + P_{PV}(t)\right) + P_e^{CHP}(t) \pm SoC_b(t) \quad (26)$$

$$P_g(t) = P_g^{CHP}(t) + P_g^B(t) \quad (27)$$

$$D_h(t) = P_h^B(t) + P_h^{CHP}(t) \quad (28)$$

2.8. Power Constraint Relations

Equation (29) represents the constraint on the electrical energy purchased from the power grid. Equation (30) represents the constraint on the gas purchased from the gas network. Equations (31) and (32) detail the constraints on the gas fuel input for the CHP and boiler. Finally, Equations (33) and (34) illustrate the constraints on the power generated by WT and Photovoltaic (PV) systems:

$$P_e^{\min} \le P_e(t) \le P_e^{\max} \tag{29}$$

$$P_g^{\min} \le P_g(t) \le P_g^{\max} \tag{30}$$

$$0 \le P_g^{CHP}(t) \le P_g^{CHP_{\max}} \tag{31}$$

$$0 \le P_g^{B}(t) \le P_g^{B_{\max}} \tag{32}$$

$$0 \le P_W(t) \le P_W^{\max} \tag{33}$$

$$0 \le P_{PV}(t) \le P_{PV}^{\max} \tag{34}$$

2.9. Demand Response

DRPs are employed to achieve lower operational costs by shifting demand from peak periods to off-peak periods. DRPs are schemes designed to encourage consumers to alter their energy consumption patterns based on energy prices throughout the day, thereby reducing their overall energy use. According to Equation (35), the difference in demand before and after the demand response should be equal to the sum of the reduced and increased demand. Additionally, as per Equation (36), the load participation factor should not exceed a certain limit. Moreover, Equation (37) stipulates that the total increase and decrease in demand over the entire operational period must be balanced [38]:

$$D(t) - \text{Load}(t) = DR(t) \cdot D(t) - L_{\text{inc}}(t) \tag{35}$$

$$DR(t) \le DR^{\max}(t) \tag{36}$$

$$\sum_t L_{\text{inc}}(t) = \sum_t DR(t) \cdot D(t) \tag{37}$$

2.10. Scenario Generation and Reduction Method

To manage the uncertainty of variables like PV and WT in stochastic planning models, scenario generation is a common approach. For this study, 1000 scenarios are created using Python, assuming a normal distribution for PV and WT. Next, a scenario reduction technique based on probability distance is utilized. This method calculates the total distance between each scenario and all others, selecting the scenario with the smallest distance as a reference. Scenarios within a specified radius are then discarded, leaving the five most representative scenarios. This procedure is visually summarized in Figure 3.

Place of Figure 3.

Uncertainty in the output of PV and WT power is modeled by Equations (38) and (39), where $P_{\text{PV},t}^{f}$ and $P_{\text{WT},t}^{f}$ represent the predicted output of PV and WT, respectively, with their associated uncertainties. $\Delta P_{\text{PV},t,s}$ and $\Delta P_{\text{WT},t,s}$ denote the errors associated with these predictions. N_T and N_s are the time interval and scenario quantities selected for modeling the uncertainty [39]:

$$P_{\text{PV},t,s} = P_{\text{PV},t}^{f} + \Delta P_{\text{PV},t,s} \quad ; \quad t = 1,\ldots,N_T; \quad s = 1,\ldots,N_s \tag{38}$$

$$P_{\text{WT},t,s} = P_{\text{WT},t}^{f} + \Delta P_{\text{WT},t,s} \quad ; \quad t = 1,\ldots,N_T; \quad s = 1,\ldots,N_s \tag{39}$$

2.11. Solution Flowchart

As shown in Figure 4, the process begins with the input data, which includes PV, WT, electrical and thermal demand, electricity and natural gas prices, and parameters related to the hub-based microgrid. To address the uncertainty in PV and WT, 1000 scenarios are generated using Python, assuming a normal distribution. Next, the probability distance method is used to reduce the scenarios to the 5 most likely ones. The optimization problem has two objectives: minimizing operational costs and reducing greenhouse gas emissions, labeled as Z_1 and Z_2 respectively. The objective function is solved using the weighted sum method, with w_1 and w_2 being the coefficients for these objectives. The system is implemented non-linearly in Python and optimized using solvers.

Place of Figure 4.

3. Simulation Results

This study considers a microgrid system that includes solar panels, a wind turbine, a CHP unit, a boiler, and an electrical energy storage system. The microgrid is connected to the power grid, purchasing and occasionally selling electrical energy. In other words, the microgrid interacts with the power grid. It is also connected to the gas network, from which it only purchases gas. The system is implemented non-linearly in Python and optimized using its solvers. All system parameters are based on references [40, 41].

Figure 5 shows the electrical demand in purple and the thermal demand in blue over a 24-hour period. The electrical demand peaks at 1350 kW during hours 13 to 21. Meanwhile, the thermal demand reaches its peak of 700 kW from hour 22 to 8 AM. During the middle of the day, thermal demand decreases but then shows an upward trend in the evening, returning to peak levels.

Place of Figure 5.

Figure 6 illustrates the price variations of electricity and heat over a 24-hour period. The price of electricity is represented in dark blue, while the price of heat is shown in yellow. As observed, energy prices fluctuate throughout the day, with a noticeable increase during peak demand hours. Specifically, from hours 13 to 21, the total energy price reaches its highest levels, driven by both electricity and heat price surges.

Place of Figure 6.

Figure 7 illustrates the gas procurement pattern of the system over a 24-hour period. Natural gas is measured in BTU, with one BTU equivalent to 293×10^{-6} kW. The system exhibits its lowest gas purchase rate of 700 kW/h during the early morning hours, from midnight to 7 AM, when demand is relatively low. In contrast, peak purchases, reaching 1680 kW/h, occur at hours 8 and 21, aligning with periods of increased energy demand. These fluctuations reflect the system's adaptive response to varying load conditions throughout the day.

Place of Figure 7.

Figure 8 shows the input power of the CHP and Boiler from gas fuel, with the CHP power depicted in red and the Boiler power in blue, both expressed in kilowatts per hour. The boiler plays a key role in meeting thermal demand, thus producing its maximum power during hours when thermal demand peaks. The CHP operates between hours 8 and 21 to generate electricity when the cost of electrical energy is high and the system requires cheaper electricity. Additionally, when thermal

demand is low, the CHP can meet the entire thermal load, allowing the boiler to be out of operation. In this system, the CHP has an electrical efficiency of 0.4 and a thermal efficiency of 0.45, while the boiler has a thermal efficiency of 0.85. For example, at hour 13, the CHP provides 384 kW/h of electrical power and 432 kW/h of thermal power, which meets the thermal demand shown in Figure 5. Additionally, the boiler provides 595 kW/h of thermal power at hour 7.

Place of Figure 8.

For solar and wind energy, 1000 scenarios were generated using the scenario generation method, which were then reduced to 5 more probable scenarios. Figure 9 shows the power output of the solar panels, and Figure 10 shows the power output of the wind turbine. Given that solar radiation reaches its maximum around noon, the PV system is capable of producing 800-1000 kW/h of electrical energy. Similarly, during hours 23 to 3, when wind speeds increase, the WT system can produce 900-1000 kW/h of electrical energy.

Place of Figure 9.

Place of Figure 10.

Figure 11 shows the electrical energy stored in the EESS. As illustrated, the stored energy in the EESS is used to meet electrical demand during hours 5-6 and 16-22, when the production of PV and WT is reduced as shown in Figures 9 and 10. On the other hand, EESS is used to take advantage of lower energy prices in the energy system. As depicted in Figure 12, EESS is charged

during hours 22-23 and 6-7, when the price of electricity is lower, and discharged during hours 4-5, 15-17, and 19-20 to help meet demand with the goal of maximizing revenue and system profit.

Place of Figure 11.

Place of Figure 12.

Figures 13 and 14 show the electrical and thermal demand after implementing the DRP. Electrical demand peaks between hours 12 and 16, while thermal demand peaks at hours 8 and 21. Figures 15 and 16 display the transferred electrical and thermal loads with the application of DRP. As observed, implementing DRP shifts loads from hours with high energy prices to hours with lower energy prices or higher shares of renewable energy.

Place of Figure 13.

Place of Figure 14.

Place of Figure 15.

Place of Figure 16.

Figure 17 shows the electrical power sold by the microgrid to the power grid in blue and the electrical power purchased by the microgrid from the power grid in red, expressed by hour. As illustrated, renewable resources reach their peak electrical power production between hours 8 and 14, during which the microgrid sells electricity to the power grid, peaking at 998.74 kW/h at hour

8. During hours 16 to 22, when electricity consumption peaks, the microgrid supplements its own resources with electricity from the power grid. Additionally, between hours 3 and 6, when the price of electricity is relatively low (as shown in Figure 5), the microgrid purchases up to 398.5 kW/h of electricity from the power grid.

Place of Figure 17.

3-1- Numerical Analysis

Based on the obtained results, Table 1 shows that the total operational cost for electrical and thermal energy using the optimized multi-carrier system is 164,682 cents. If the electrical and thermal demand were met solely through the power and gas grid, the total cost would be 279,910 cents. This represents approximately a 41% savings. Additionally, the amount of pollution produced by the optimized system is 18,124.4 kilograms.

Place of Table 1.

According to Figure 16, during hours 8 to 12, when electrical demand is low, and as shown in Figure 8, PV systems are at their maximum production capacity due to peak solar radiation. Table 2 indicates that during these hours, the total power produced by renewable sources not only meets the electrical demand but also maximizes the sale of electricity to the grid, generating revenue. Consequently, the microgrid can operate as 100% renewable during certain hours of the day, leading to both energy savings and revenue generation, while also contributing to environmental protection by reducing greenhouse gas emissions.

Place of Table 2.

3-2- Sensitivity Analysis

Table 3 shows the impact of varying the objective function coefficients on the operational cost and greenhouse gas emissions. As the coefficient of the first objective function increases, the coefficient of the second objective function decreases, since their sum always equals one. Furthermore, increasing the coefficient of any objective function signifies a higher importance placed on that objective in the optimization process. Thus, the operational cost and emissions exhibit an inverse relationship with their respective coefficients.

Place of Table 3.

Table 4 shows the effect of varying the load of different resources on greenhouse gas emissions. The table separately examines the impact of reducing the load by 30% to 10% for CHP, the boiler, the electricity grid, and the gas network, while keeping other resources constant. As indicated, the gas network results in the highest emissions, whereas the electricity grid results in the lowest emissions.

Place of Table 4.

4- Conclusion

This study presents a comprehensive approach to optimizing a hub-based microgrid system that integrates renewable energy resources, such as solar and wind, with traditional energy sources like CHP units and boilers. By incorporating a DRP and addressing the uncertainty inherent in renewable energy production through a scenario generation and reduction method, the proposed model effectively balances both electrical and thermal demands. The bi-objective optimization framework, focusing on operational cost minimization and greenhouse gas emissions reduction, demonstrates significant benefits in terms of economic feasibility and environmental impact. The results indicate a 41% cost reduction when compared to a conventional energy supply from the

grid, highlighting the potential for cost-efficient energy management. Furthermore, the system's ability to operate solely on renewable energy during specific hours of the day, coupled with the optimization of electricity sales to the grid, demonstrates its capability to generate revenue while contributing to environmental sustainability. The sensitivity analysis confirms the robustness of the model, showing how varying the importance of each objective function can lead to optimal trade-offs between cost reduction and emission minimization. The proposed microgrid system provides a solid foundation for future research, with opportunities to incorporate hydrogen-based technologies and electric vehicles into the system's framework. These additions could further enhance the system's performance and sustainability, paving the way for more resilient and eco-friendly energy management solutions in the future.

Author Contributions:

Mohammad amin Babajani-Chari: Conceptualization, Methodology, Software, Formal analysis, Investigation, Data Curation, Writing - Original Draft, Visualization.

Ali Ghasemi-Marzbali: Conceptualization, Methodology, Formal analysis, Investigation, Data Curation, Writing - Original Draft, Writing - Review & Editing, Visualization, Supervision.

Funding:

Not applicable.

Data Availability:

The data generated or analyzed during this study are included within the published article or cited accordingly.

Conflict of interest:

The authors declare that they have no known competing financial interests or personal relationships that could have appeared to influence the work reported in this paper.

Human Participants and/or Animals:

Not applicable.

Ethical approval:

Not applicable.

Acknowledgment:

Not applicable.

Declaration of Competing Interest

The authors declare that they have no known competing financial interests or personal relationships that could have appeared to influence the work reported in this paper.

References

[1] Gholitabar, O., and Ghasemi-Marzbali, A. "Introduction and literature review to deployment of photovoltaic systems in buildings", Natural Energy, Lighting, and Ventilation in Sustainable Buildings, 45-64 (2023). DOI: https://doi.org/10.1007/978-3-031-41148-9_3.

[2] Abedinia, O., Ghasemi-Marzbali, A., Gouran-Orimi, et al. "Presence of renewable resources in a smart city for supplying clean and sustainable energy", In Decision making using AI in energy

and sustainability: methods and models for policy and practice (pp. 233-251). Cham: Springer International Publishing (2023). DOI: https://doi.org/10.1007/978-3-031-38387-8_14.

[3] Moazzen, F., and Hossain, M. J. "A two-layer strategy for sustainable energy management of microgrid clusters with embedded energy storage system and demand-side flexibility provision", Applied Energy, 377, 124659 (2025). DOI: https://doi.org/10.1016/j.apenergy.2024.124659.

[4] Riki, A., Oukati Sadegh, M., and Narouei, O. "Flexibility-constrained energy management of smart energy hubs considering peer to peer transactive energy and demand response program", International Journal of Industrial Electronics Control and Optimization, 8(1), pp. 67-82 (2025). DOI: https://doi.org/10.22111/ieco.2024.49216.1587.

[5] Yan, L., Lyu, L., and Niu, Q. "Towards efficient energy hubs: two-stage robust optimization with compressed air storage, electric vehicles and renewable energy integration," Journal of Energy Storage, 111, 115338 (2025). DOI: https://doi.org/10.1016/j.est.2025.115338.

[6] Wang, C., Wang, M., Wang, A., et al. "Multiagent deep reinforcement learning-based cooperative optimal operation with strong scalability for residential microgrid clusters", Energy, 314, 134165 (2025). DOI: https://doi.org/10.1016/j.energy.2024.134165.

[7] Chen, Q., and Yin, X. "Sustainable coastal energy development: integrated modeling of renewable energy sources for optimal economic and environmental performance", Energy, 134504 (2025). DOI: https://doi.org/10.1016/j.energy.2025.134504.

[8] Ghasemi-Marzbali, A., Shafiei, M., and Ahmadiahangar, R. "Day-ahead economical planning of multi-vector energy district considering demand response program", Applied Energy, 332, 120351 (2023). DOI: https://doi.org/10.1016/j.apenergy.2022.120351.

[9] Ebrahimi, H., Yazdaninejadi, A., and Golshannavaz, S. “Decentralized prioritization of demand response programs in multi-area power grids based on the security considerations”, ISA transactions, 134, 396-408 (2023). DOI: https://doi.org/10.1016/j.isatra.2022.07.031.

[10] Dey, B., Sharma, G., Bokoro, P. N., et al. “An intelligent incentive-based demand response program for exhaustive environment constrained techno-economic analysis of microgrid system”, Scientific Reports, 15(1), 894 (2025). DOI: https://doi.org/10.1038/s41598-025-85175-z.

[11] Hai, T., Singh, N. S. S., and Jamal, F. “Energy management of a microgrid with integration of renewable energy sources considering energy storage systems with electricity price”, Journal of Energy Storage, 110, 115191 (2025). DOI: https://doi.org/10.1016/j.est.2024.115191.

[12] Huang, J. C., Cheng, H. C., Shu, M. H., et al. “Market-based optimization of integrated energy systems: modeling and analysis of multi-carrier energy networks”, Electric Power Systems Research, 239, 111245 (2025). DOI: https://doi.org/10.1016/j.epsr.2024.111245.

[13] Karimi, H., Jadid, S., and Hasanzadeh, S. “Optimal-sustainable multi-energy management of microgrid systems considering integration of renewable energy resources: a multi-layer four-objective optimization,” Sustainable Production and Consumption, 36, pp. 126-138 (2023). DOI: https://doi.org/10.1016/j.spc.2022.12.025.

[14] Moniruzzaman, M., Yassine, A., and Benlamri, R. “Blockchain and cooperative game theory for peer-to-peer energy trading in smart grids”, International Journal of Electrical Power & Energy Systems, 151, 109111 (2023). DOI: https://doi.org/10.1016/j.ijepes.2023.109111.

[15] Assad, U., Hassan, M. A. S., Farooq, U., et al. “Smart grid, demand response and optimization: a critical review of computational methods”, Energies, 15(6), 2003 (2022). DOI: https://doi.org/10.3390/en15062003.

[16] Al-Humaid, Y. M., Khan, K. A., Abdulgalil, et al. “Two-stage stochastic optimization of sodium-sulfur energy storage technology in hybrid renewable power systems”, IEEE Access, 9, 162962-162972 (2021). DOI: 10.1109/ACCESS.2021.3133261.

[17] Strach, D. M. “Development of operating and pricing concepts for the V2G provision of an EV aggregator through a bi-level dynamic stackelberg optimization”, Master's Thesis, Universitat Politècnica de València, (2024). DOI: http://hdl.handle.net/10251/212849.

[18] Güven, A. F., and Mengi, O. Ö. “Assessing metaheuristic algorithms in determining dimensions of hybrid energy systems for isolated rural environments: exploring renewable energy systems with hydrogen storage features”, Journal of Cleaner Production, 428, 139339 (2023). DOI: https://doi.org/10.1016/j.jclepro.2023.139339.

[19] Elsisi, M., Amer, M., and Su, C. L. “A comprehensive review of machine learning and IoT solutions for demand side energy management, conservation, and resilient operation”, Energy, 128256 (2023). DOI: https://doi.org/10.1016/j.energy.2023.128256.

[20] Niu, Q., You, M., Yang, Z., et al. “Economic emission dispatch considering renewable energy resources—a multi-objective cross entropy optimization approach”, Sustainability, 13(10), 5386 (2021). DOI: https://doi.org/10.3390/su13105386.

[21] Zhang, Z., Huang, Y., Chen, Z., et al. “Integrated demand response for microgrids with incentive compatible bidding mechanism”, IEEE Transactions on Industry Applications, 59(1), pp. 118-127 (2022). DOI: 10.1109/TIA.2022.3204626.

[22] Muhtadi, A., Pandit, D., Nguyen, N., et al. “Distributed energy resources based microgrid: review of architecture, control, and reliability”, IEEE Transactions on Industry Applications, 57(3), pp. 2223-2235 (2021). DOI: 10.1109/TIA.2021.3065329.

[23] Arumugham, V., Ghanimi, H. M., Pustokhin, et al. “An artificial-intelligence-based renewable energy prediction program for demand-side management in smart grids”, Sustainability, 15(6), 5453 (2023). DOI: https://doi.org/10.3390/su15065453.

[24] Kim, H. J., and Kim, M. K. “Risk-based hybrid energy management with developing bidding strategy and advanced demand response of grid-connected microgrid based on stochastic/information gap decision theory”, International Journal of Electrical Power & Energy Systems, 131, 107046 (2021). DOI: https://doi.org/10.1016/j.ijepes.2021.107046.

[25] Kumari, A., Chintukumar Sukharamwala, U., Tanwar, S., et al. “Blockchain-based peer-to-peer transactive energy management scheme for smart grid system”, Sensors, 22(13), 4826 (2022). DOI: https://doi.org/10.3390/s22134826.

[26] Yang, C., Sun, Y., Zou, Y., et al. “Optimal power flow in distribution network: a review on problem formulation and optimization methods”, Energies, 16(16), 5974 (2023). DOI: https://doi.org/10.3390/en16165974.

[27] Alamir, N., Kamel, S., Megahed, T. F., et al. “A multi-layer techno-economic-environmental energy management optimization in cooperative multi-microgrids with demand response program and uncertainties consideration”, Scientific Reports, 14(1), 23418 (2024). DOI: https://doi.org/10.1038/s41598-024-72706-3.

[28] Rahman, S., Khan, I. A., Khan, et al. “Comprehensive review & impact analysis of integrating projected electric vehicle charging load to the existing low voltage distribution system”, Renewable and Sustainable Energy Reviews, 153, 111756 (2022). DOI: https://doi.org/10.1016/j.rser.2021.111756.

[29] Wang, J., Gao, Y., and Li, R. “Reinforcement learning based bilevel real-time pricing strategy for a smart grid with distributed energy resources”, Applied Soft Computing, 155, 111474 (2024). DOI: https://doi.org/10.1016/j.asoc.2024.111474.

[30] Shafiei, K., Zadeh, S. G., and Hagh, M. T. “Planning for a network system with renewable resources and battery energy storage, focused on enhancing resilience”, Journal of Energy Storage, 87, 111339 (2024). DOI: https://doi.org/10.1016/j.est.2024.111339.

[31] Azeem, O., Ali, M., Abbas, G., et al. “A comprehensive review on integration challenges, optimization techniques and control strategies of hybrid AC/DC Microgrid”, Applied Sciences, 11(14), 6242 (2021). DOI: https://doi.org/10.3390/app11146242.

[32] Wang, Q., Hou, Z., Guo, Y., et al. “Enhancing energy transition through sector coupling: a review of technologies and models”, Energies, 16(13), 5226 (2023). DOI: https://doi.org/10.3390/en16135226.

[33] Rakipour, D., and Barati, H. “Probabilistic optimization in operation of energy hub with participation of renewable energy resources and demand response”, Energy, 173, pp. 384-399 (2019). DOI: https://doi.org/10.1016/j.energy.2019.02.021.

[34] Ko, W., and Kim, J. “Generation expansion planning model for integrated energy system considering feasible operation region and generation efficiency of combined heat and power”, Energies, 12(2), 226 (2019). DOI: https://doi.org/10.3390/en12020226.

[35] Lin, K. W., and Wu, H. W. “Emissions and energy/exergy efficiency in an industrial boiler with biodiesel and other fuels”, Case Studies in Thermal Engineering, 50, 103474 (2023). DOI: https://doi.org/10.1016/j.csite.2023.103474.

[36] Faraji, J., Hashemi-Dezaki, H., and Ketabi, A. “Optimal probabilistic scenario-based operation and scheduling of prosumer microgrids considering uncertainties of renewable energy

sources", Energy Science & Engineering, 8(11), pp. 3942-3960 (2020). DOI: https://doi.org/10.1002/ese3.788.

[37] Ghasemi-Marzbali, A., Ahmadiahangar, R., Orimi, S. G., et al. "Energy management of an isolated microgrid: a practical case", In IECON 2021–47th Annual Conference of the IEEE Industrial Electronics Society (pp. 1-6). IEEE, (2021). DOI: 10.1109/IECON48115.2021.9589801.

[38] Siahchehre Kholerdi, S., and Ghasemi-Marzbali, A. "Effect of demand response programs on industrial specific energy consumption: study at three cement plants", International Transactions on Electrical Energy Systems, 2022(1), 8550927 (2022). DOI: https://doi.org/10.1155/2022/8550927.

[39] Kumar, R. S., Raghav, L. P., Raju, et al. "Intelligent demand side management for optimal energy scheduling of grid connected microgrids", Applied Energy, 285, 116435 (2021). DOI: https://doi.org/10.1016/j.apenergy.2021.116435.

[40] Nojavan, S., Zare, K., and Mohammadi-Ivatloo, B. "Application of fuel cell and electrolyzer as hydrogen energy storage system in energy management of electricity energy retailer in the presence of the renewable energy sources and plug-in electric vehicles", Energy conversion and management, 136, pp. 404-417 (2017). DOI: https://doi.org/10.1016/j.enconman.2017.01.017.

[41] Imeni, M. L., Ghazizadeh, M. S., Lasemi, M. A., et al. "Optimal scheduling of a hydrogen-based energy hub considering a stochastic multi-attribute decision-making approach", Energies, 16(2), 631 (2023). DOI: https://doi.org/10.3390/en16020631.

Mohammad amin Babajani-Chari received his M.Sc. degree in Electrical Engineering from Mazandaran University of Science and Technology, Iran, in 2024. His research interests include microgrids, power system planning, renewable energy, and smart grids.

Ali Ghasemi-Marzbali (Known as Ali Ghasemi) received the B.S., M.S. and Ph.D all in electrical engineering with honor in 2009, 2011 and 2017, from IUT and UMA, respectively. He is currently an Associate Professor in Mazandaran University of Science and Technology (USTMB), Iran. He has published over 200 papers in international journals and conference proceedings. His research interests span control, operation, planning, economics, and regulation of electric energy systems. He is a member of the IAEEE. He has been listed at times by Thomson Reuters among the world's top 2% researchers in engineering and has received several awards for his research and publications, including young researcher and best paper awards.

List of figure:

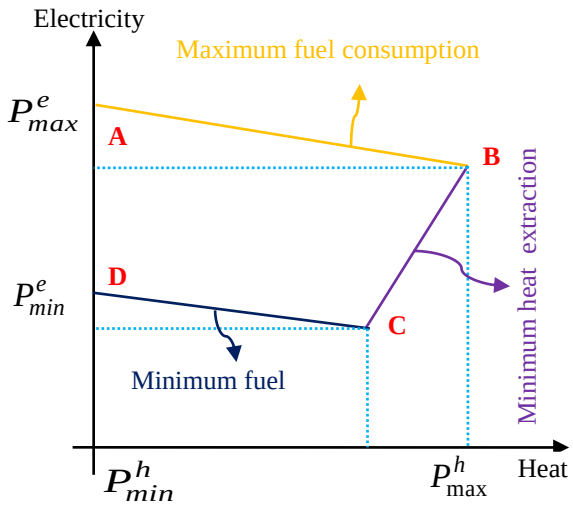

Figure 1- CHP Feasible Operating Region

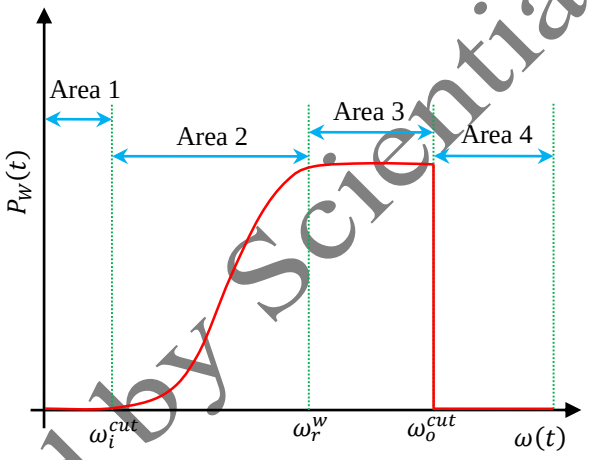

Figure 2. Wind Turbine Power Output

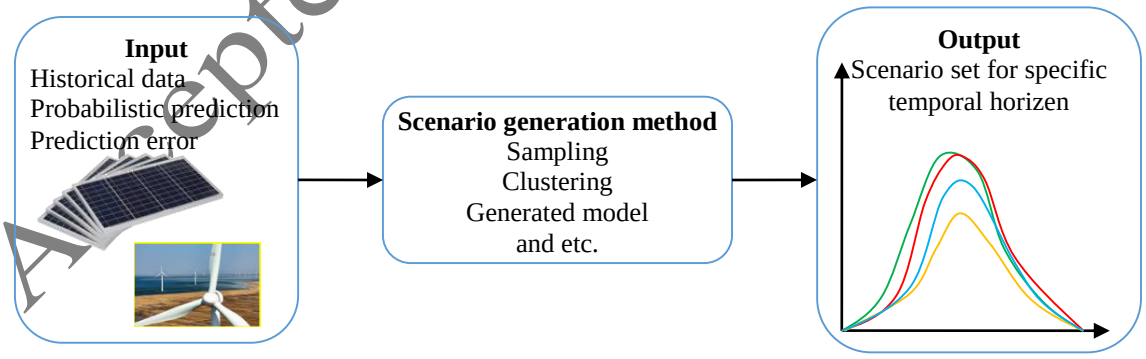

Figure 3. Overall Framework of the Scenario Generation Process

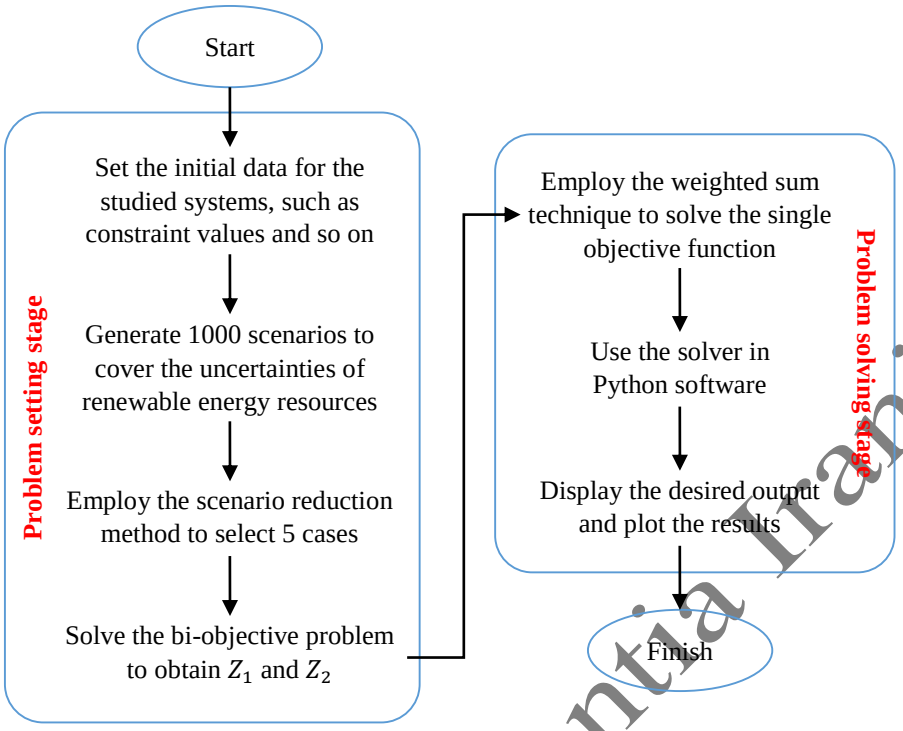

Figure 4. Optimization Process Flowchart

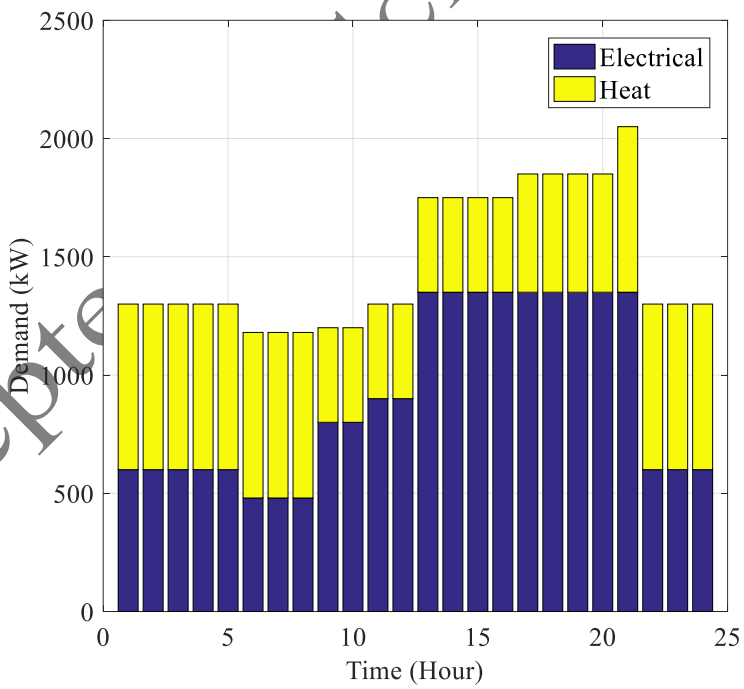

Figure 5. Electrical and Thermal Demand

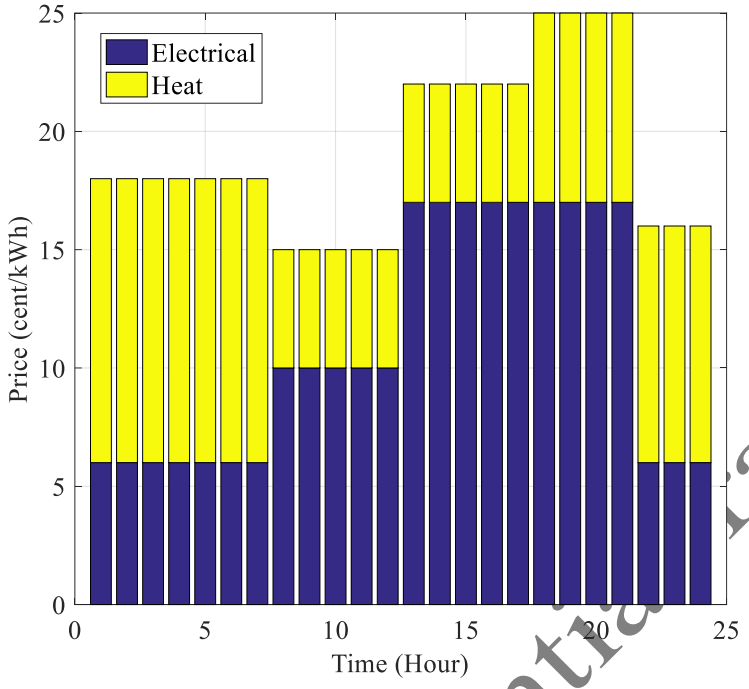

Figure 6. Electricity and Gas Prices Purchased from the Grid

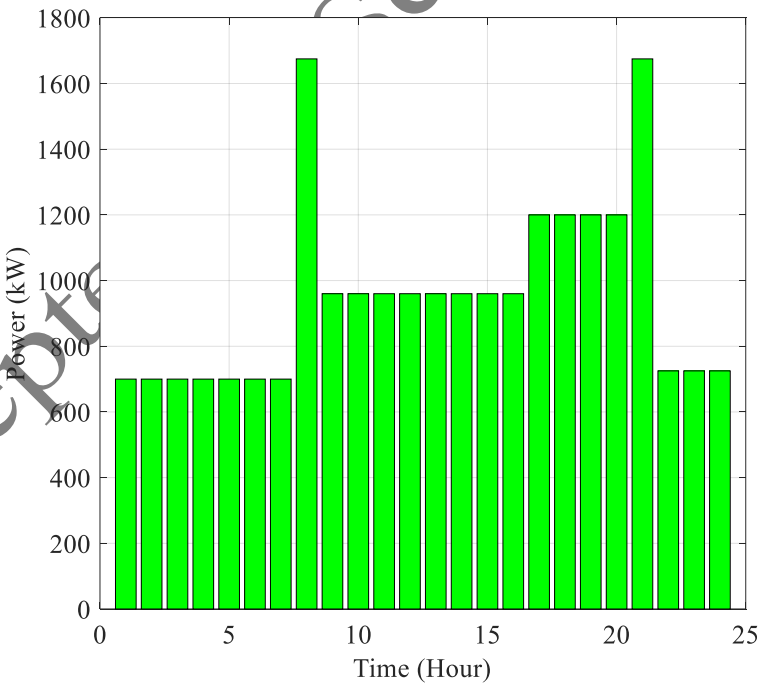

Figure 7. Amount of Gas Purchased from the Gas Network

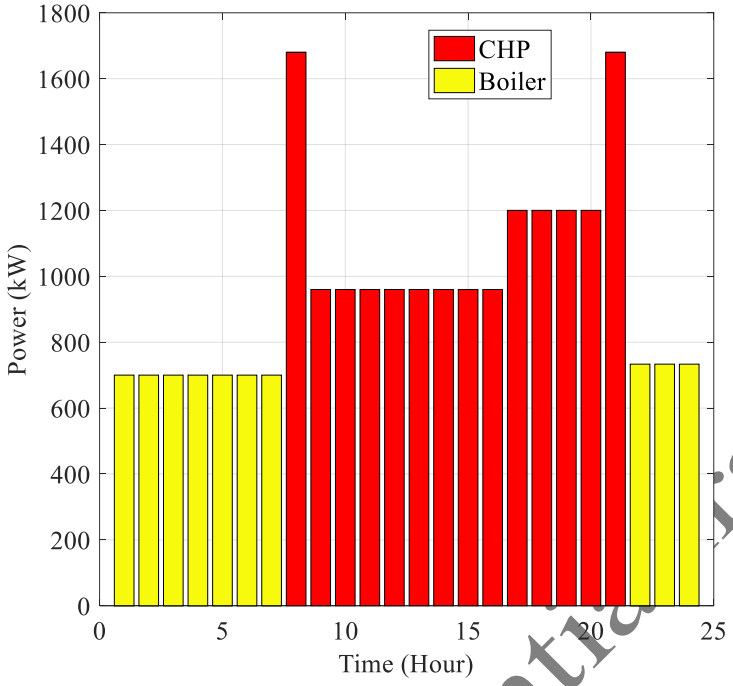

Figure 8. Input Fuel to CHP and Boiler

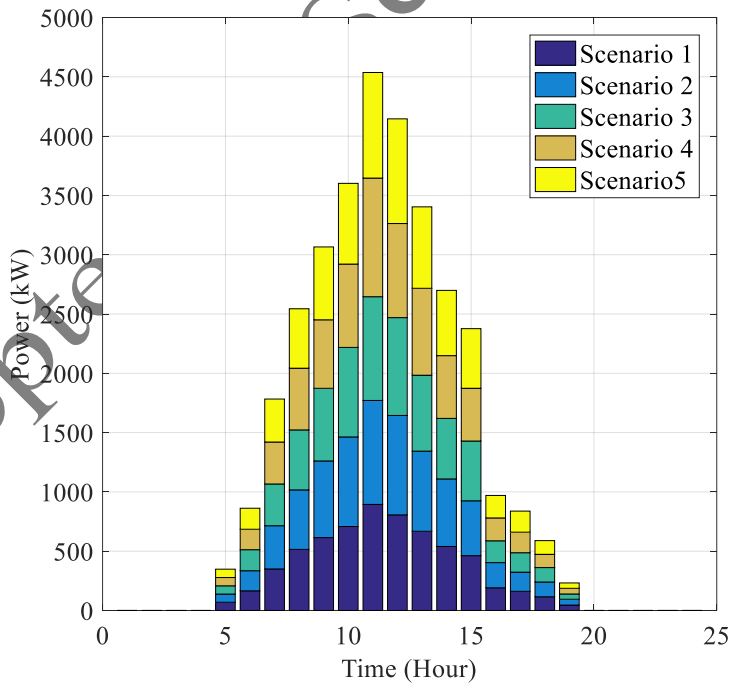

Figure 9. Solar Panel Power Output

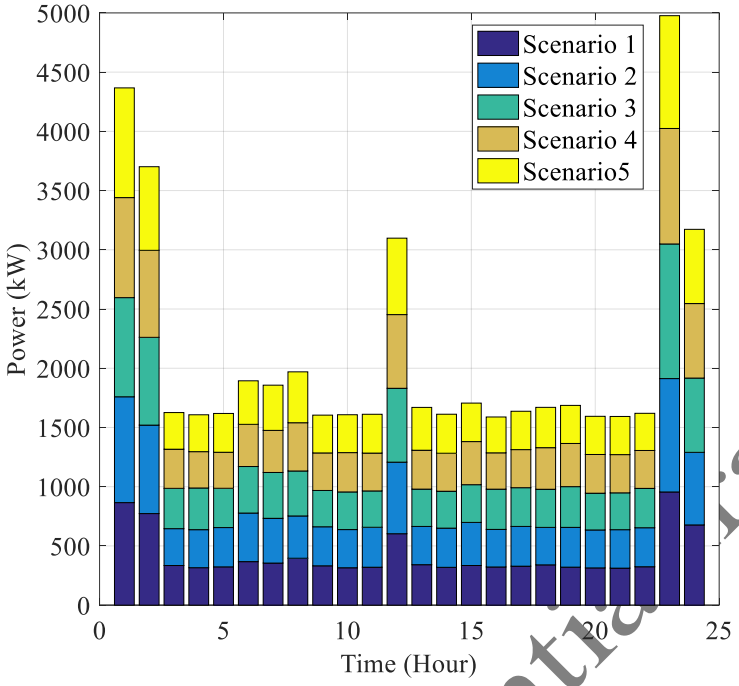

Figure 10. Wind Turbine Power Output

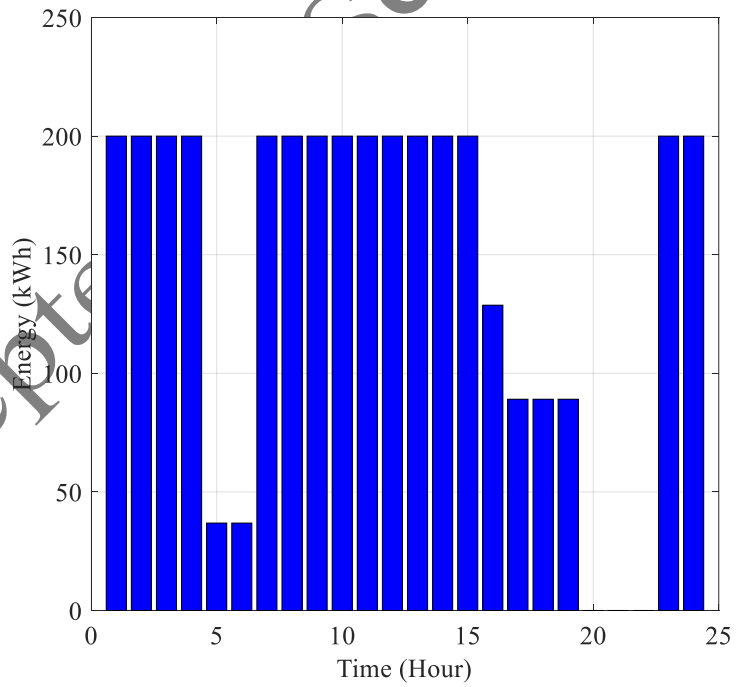

Figure 11. Energy Stored in EESS

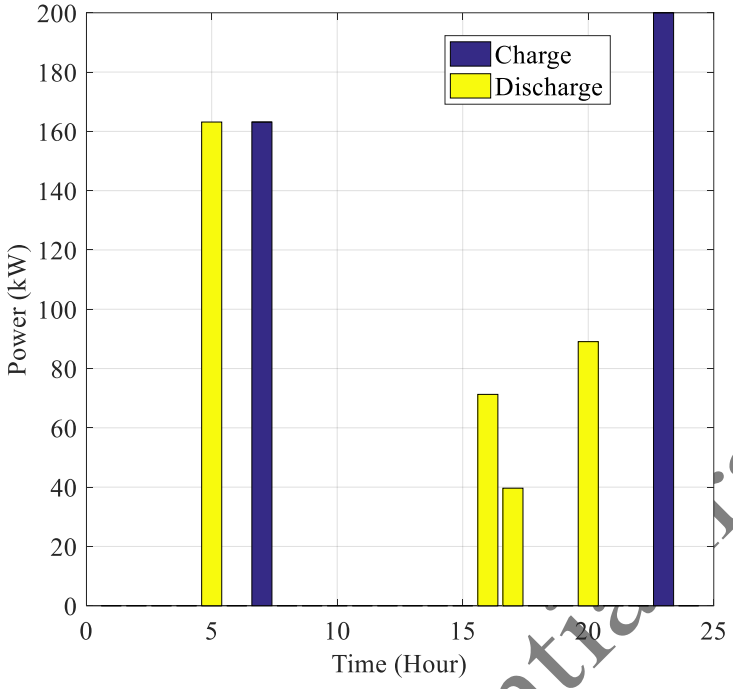

Figure 12. Charging and Discharging of EESS

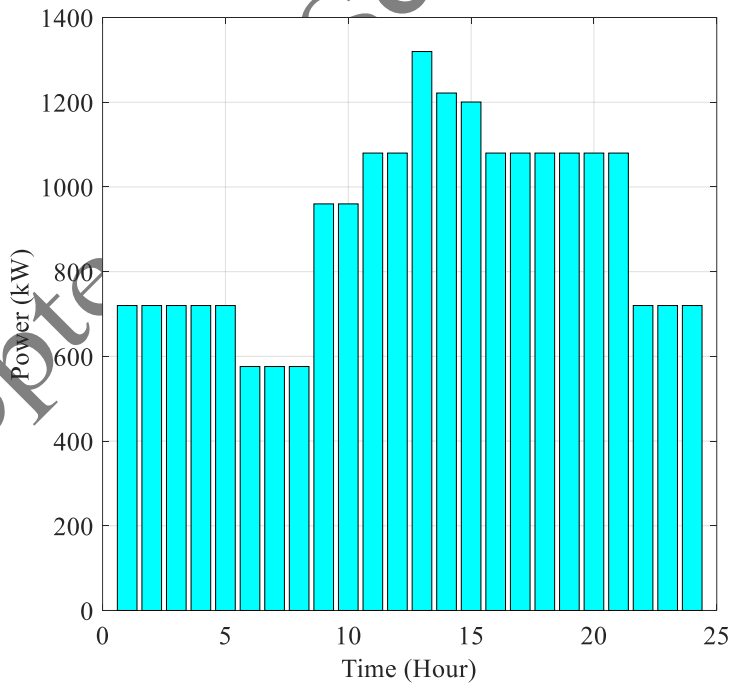

Figure 13. Electrical Demand After DRP

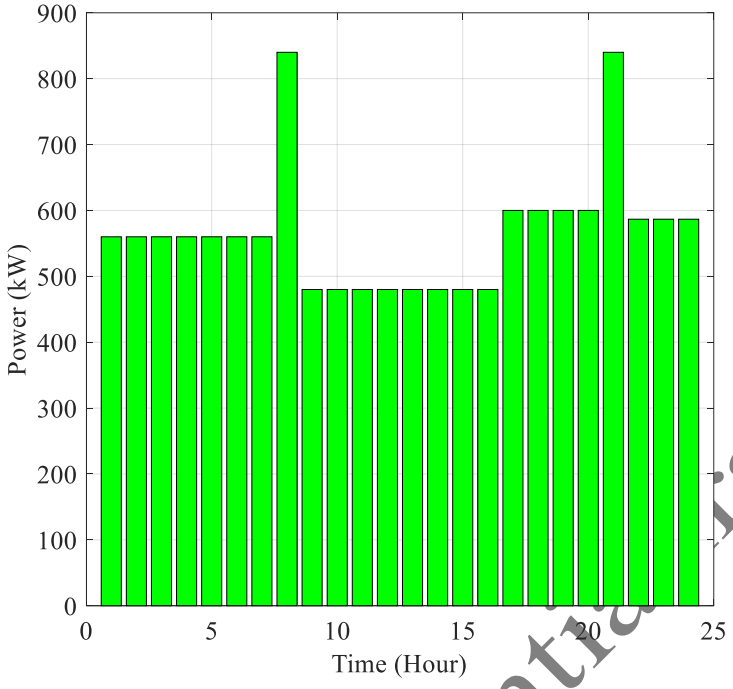

Figure 14. Thermal Demand After DRP

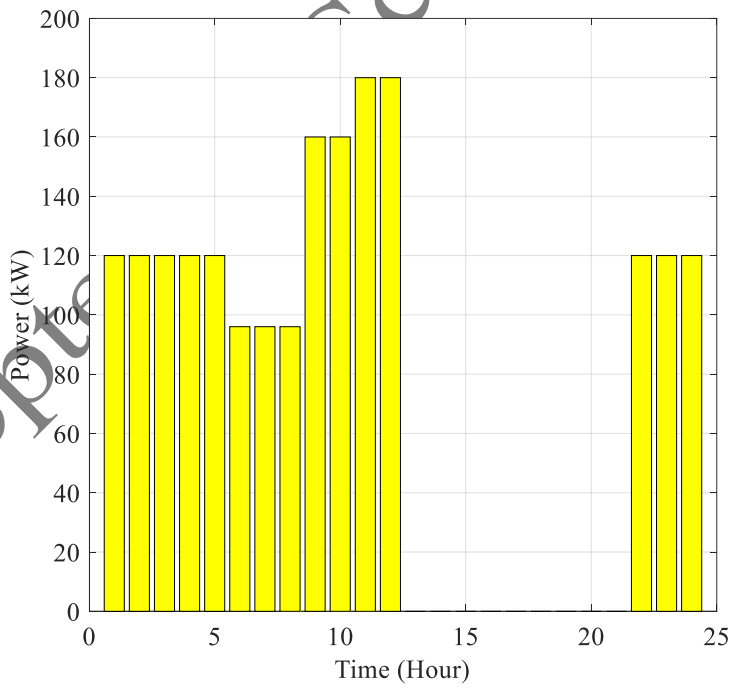

Figure 15. Transferred Electrical Load After DRP

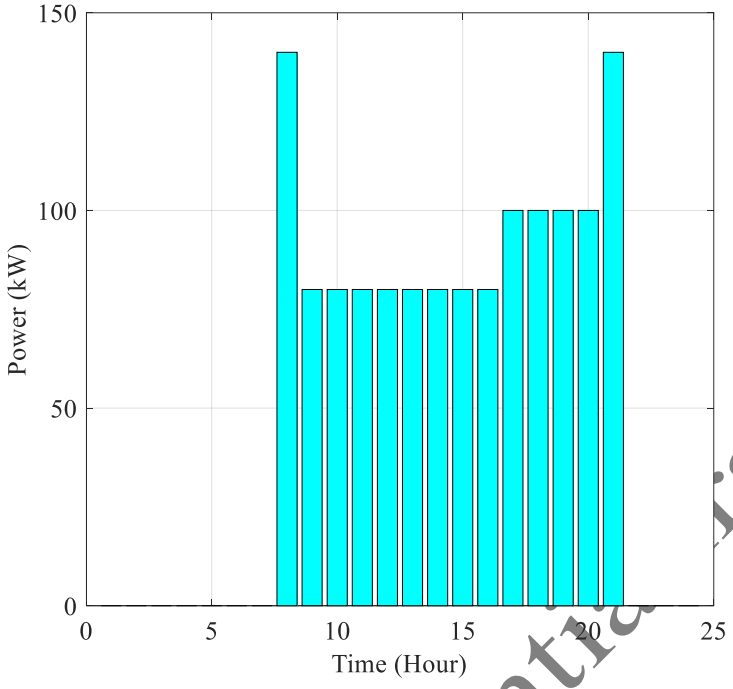

Figure 16. Transferred Thermal Load After DRP

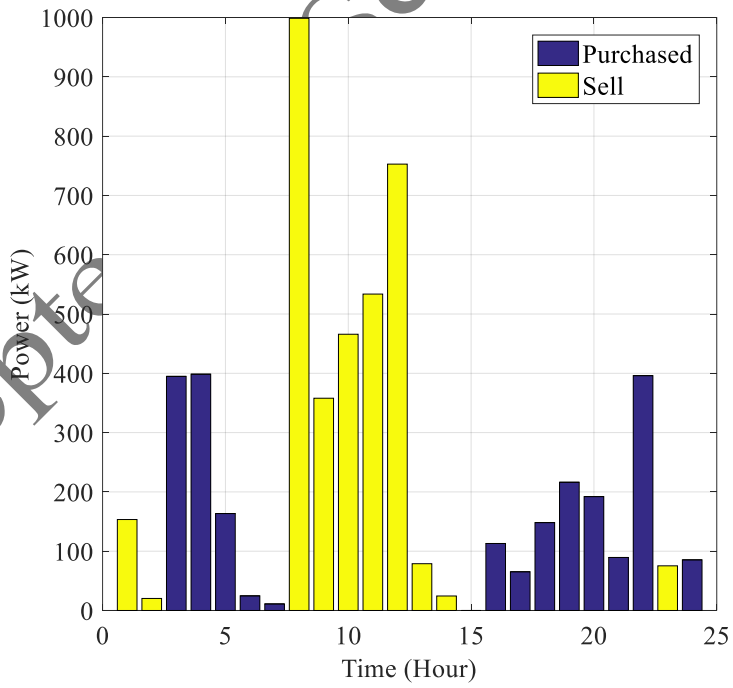

Figure 17. Electrical Energy Purchased from and Sold to the Power Grid

List of figure:

List of Tables

Table 1. Objective Function Results with DRP

w_1	w_2	Operation Cost (Cents)	Emission (kg)
0.5	0.5	164,682.29	18,124.42

Table 2. Comparison of Demand, Production by RER, and Electricity Sales

Hour (h)	8	9	10	11	12
Demand (kW)	480	800	800	900	900
PV (kW)	509	613	720	908	829
WT (kW)	393	320	321	322	619
E-Sold (kW)	422	133	401	330	548

Table 3. Sensitivity Analysis of Objective Function Coefficients

Case	w_1	w_2	Operation Cost (Cents)	Emission (kg)
1	0.9	0.1	112,809.37	23,374.19
2	0.8	0.2	125,277.60	22,561.74
3	0.7	0.3	141,745.83	20,749.30
4	0.6	0.4	158,214.06	19,936.86
5	0.5	0.5	164,682.29	18,124.42
6	0.4	0.6	176,462.49	16,571.92
7	0.3	0.7	181,150.51	16,552.74
8	0.2	0.8	187,905.29	16,480.07
9	0.1	0.9	221,513.29	15,260.10

Table 4. Impact of Load Reduction on Greenhouse Gas Emissions

Source	Load Change	Emission (kg)
CHP	-10%	17,649.22
	-20%	17,174.02
	-30%	16,698.82
Boiler	-10%	17,911.42
	-20%	17,698.42
	-30%	17,485.42
Electrical Grid	-10%	18,032.48
	-20%	17,940.53
	-30%	17,848.59
Gas Grid	-10%	17,092.12
	-20%	16,059.82
	-30%	15,027.52